

Project final report

Graphene assisted terahertz modulators

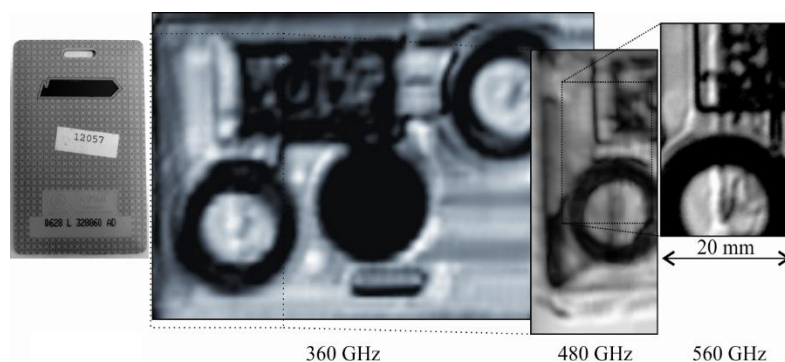
NKFI-ID: 109674

Project leader: Péter Földesy

Period: 2013-09-01 - 2017-08-31

Introduction

The topic of the project is to use sub-THz radiation for imaging. The sub-THz (0.4-2 mm wavelength or 200 GHz-1 THz) radiation is electronically detectable, while its free space behavior is similar to smaller wavelength radiation, like the visible range. Due to the relatively large wavelength compared to thermal, IR, visible radiation the imager construction is not trivial, meaning that a reasonable image size (e.g. QCIF) would take about $30 \times 24 \text{ cm}^2$, which is prohibitive in the practice considering manufacturing cost, optical focusing and lens selection. The common practice is some form of mechanical scanning using a limited number of sensors. We aimed to investigate the possibility of constructing electrically changeable solid state free space modulators. We have explored different techniques, both electrically and optically controllable setups. We aimed to investigate the topic from various directions keeping in mind, that the image formation, sensory technology, and application fields are the goals behind.



One of our mechanically raster scanned sub-THz image sequence at different frequencies of the same entry card.

Modulator experiments

The feasibility of graphene assisted sub-THz modulators has been demonstrated from several aspects [2]. An outstanding performance is presented in [Seung Hoon Lee et al. “Switching terahertz waves with gate-controlled active graphene metamaterials”, *Nature Materials* 11, 936–941 (2012)] reporting to modulate both the amplitude of the transmitted wave by up to 90% (10 dB) and its phase by more than 40 degrees at room temperature. As a further direction [Yan, Rusen and Arezoomandan et al., „Exceptional terahertz wave modulation in graphene enhanced by frequency selective surfaces”, *ACS Photonics* 3 (3), pp. 315-323., 2016], concluded that a pair of self-gated 2D semiconductors is employed as the active material instead of graphene, near-zero insertion loss can be achieved, thus approaching the ideal modulator performance: less than 0.5 dB insertion loss with more than 90% modulation depth. Though these recent

results are impressive, the modulators suffer from relatively low modulation depth, low spatial resolution, and limited phase shifting capabilities.

The modulation depth is typically given by $100 * (T_{max}/T_{min})$ or in logarithmic scale. THz transmission may reach as much as 50-60% absorption ratio when the unstructured graphene sheet conductivity is reduced to a practical limit. To reach it, very high electric field required (>200V) with dielectric isolation is required, which electric field is limited by the structure breakdown voltage.

Our modulation efforts focused on electrically and optically switchable solutions. In our experimentation, commercially available graphene sheets were used and postprocessed. The structuring the sheets have been done by dry reactive ion etching and optical lithography. The related microwave structures and antenna development, matching in various experiments is performed by an EM simulator (CST). The first investigated topic has been the amplitude and phase modulation by graphene and other standard microtechnology material structures. Si-SiO₂-graphene 4x4 and other sized modulation arrays has been manufactured (PMMA transferred monolayer graphene onto Si-SiO₂ layers, optical lithography and O₂-Ar plasma etching, finally titan adhesive layer and gold wire contacting). In order to enhance the light-matter interactions between the THz waves and graphene, thus potential modulation depth, resonant structures has been implemented such as Fabry-Perot cavities or metamaterials. During the manufacturing trials, we found out that the graphene's adhesion to the Si and SiO₂ surfaces is very low, and the structured material drifted and relocated on the Si or SiO₂ surfaces, resulting in low yield even at small arrays.

Regarding the application requirements, high modulation depth (>7 dB or 80% modulation depth) is preferable for most single channel/pixel applications (e.g. high data-rate interconnects). As the modulator integrated into an array, the overall image forming accumulate the non-filtered transmission, including unwanted pixel values and noise (e.g. compressed sensing). Thus, the modulator requires higher performance to result in better images. In general, the modulation depth gives a clue for the achievable final image quality (bit-depth), regardless of the modulation and denoising scheme. As a conclusion of this investigation and trials we faced that the graphene based modulator array may result in unacceptable image quality, control circuitry and physical size, beside the technological difficulties.

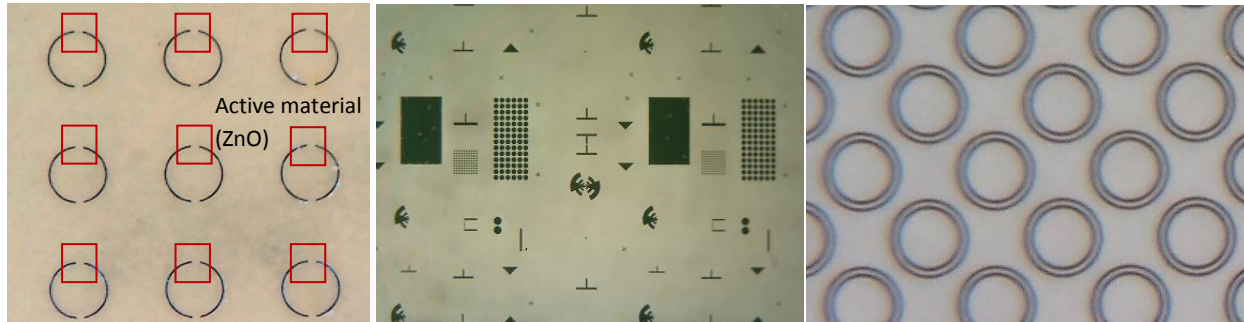
In order to improve the modulation depth and investigate the possible sensor and modulator integration, several architectures have been designed and manufactured using not only graphene as active material:

- PDMS and SU8 thermoelastic structures in Fabry-Pérot alignment with IR optical readout,
- resonating cantilevers and bridges in also Fabry-Pérot and Gires-Tournois alignment, and
- 2D and 2.5D metamaterials.
- FET based active resonators.

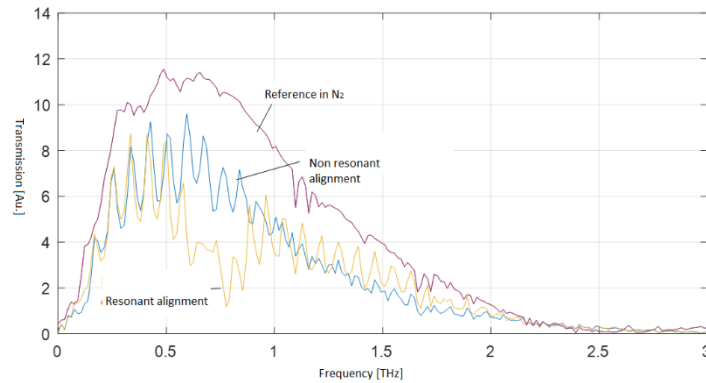
We manufactured and measured the performance the different setups. Due to the difficulties to integrate graphene on bare or structured surfaces, we changed the active material to the better known ZnO. The choice of ZnO was due to it is a wide-bandgap semiconductor of the II-VI semiconductor group. The active material has been deposited on boron glass and also on silicon wafers with metal antenna structures of Ti/Au composition. In order to improve the effect of conductivity change of the active elements, the metallic structures has been not only electrically connected measurement points, but arranged in metamaterial structures (meaning periodic element array of larger than appr. 10x10 identical elements).

We investigated the commonly selected periodic structures asymmetric periodic structures (split ring array) and especially those, which show fano-resonance (e.g. asymmetric split ring array) including novel arrangements.

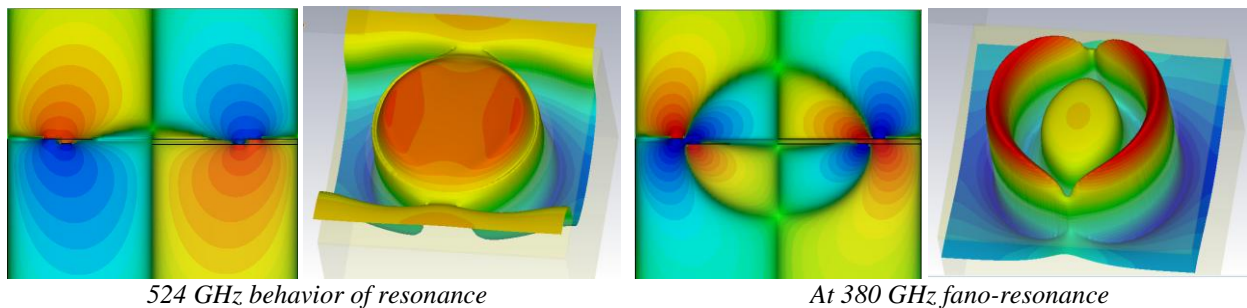
The measurements have been performed in continuous wave radiation source (260-750 GHz) in the MTA-EK-MFA laboratory and using time domain spectroscopy (300 GHz – 3 THz) with the courtesy of University of Pécs, Institute of Physics.



Experimental arrangements: (left) asymmetric split ring resonator showing fano-resonance with ZnO active materials, (middle) resonant and periodic antenna structures with graphene and ZnO active materials, (right) 2.5D asymmetric substrate-metal-dielectric-metal metamaterial resonators with thermoelastic dielectric.



Modulation experiment time domain spectroscopy measurement results of resonant and non-resonant alignment (parallel and orthogonal polarization directions) of asymmetric split ring resonators.



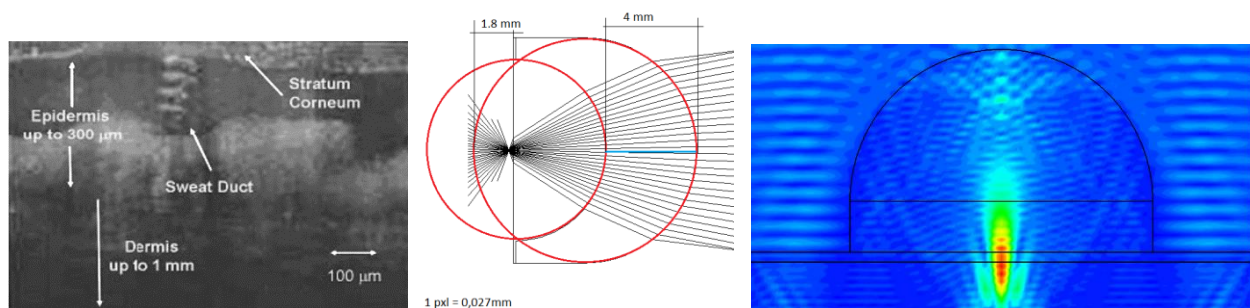
EM simulation results of the asymmetric substrate-metal-dielectric-metal metamaterial resonators under linearly polarized radiation.

Biological application

The reached modulation depth and control was not satisfactory enough for imaging due to manufacturing difficulties, thus we stepped towards the applications in the experiments and research in parallel of modulator trials. The main application field was phase sensitive imaging and sub-THz absorption microscopy of the human skin with a combination of visible light image fusion of CMOS camera images. More precisely, phase sensitive, broadband (240-520 GHz), circularly polarized scanning microscopy based on glycerin immersion and silicon lens with mechanical scanning instead of the planned electronic modulation.

The topic was to monitor a phenomena in which the human skin microwave absorbance changes under various stimuli and localize its source in the microscopic regime. The nature of microwave absorbance change under mental and physiological stimuli (e.g. stress) is investigated and presented in various publications, but its exact description is still missing (the phenomena is explained in e.g. Vorobyov, Alexander, et al. "Human physical condition RF sensing at THz range." Engineering in Medicine and Biology Society (EMBC), 2016 IEEE 38th International Conference, 2016. and in <https://www.ncbi.nlm.nih.gov/pmc/articles/PMC4357862/>). The skin ducts goes through the epidermis to the surface of the stratum corneum in a helical form. Due to the sweat these helical ducts are filled with the conducting liquid and behaves as a low quality circularly polarized antennas in the 400-600 GHz range. This assumption has been proved partially on large surface areas, though the publications had not separated the skin duct resonance from the large scale uniform wet skin absorbance. In order to find the real source of this important effect, we have developed a multimodal microscope. The microscopic setup is reasonable because the used wavelength is 600-700 μm and the skin duct size is near only 100 μm . Thus, sub-wavelength imaging is required to observe individual ducts.

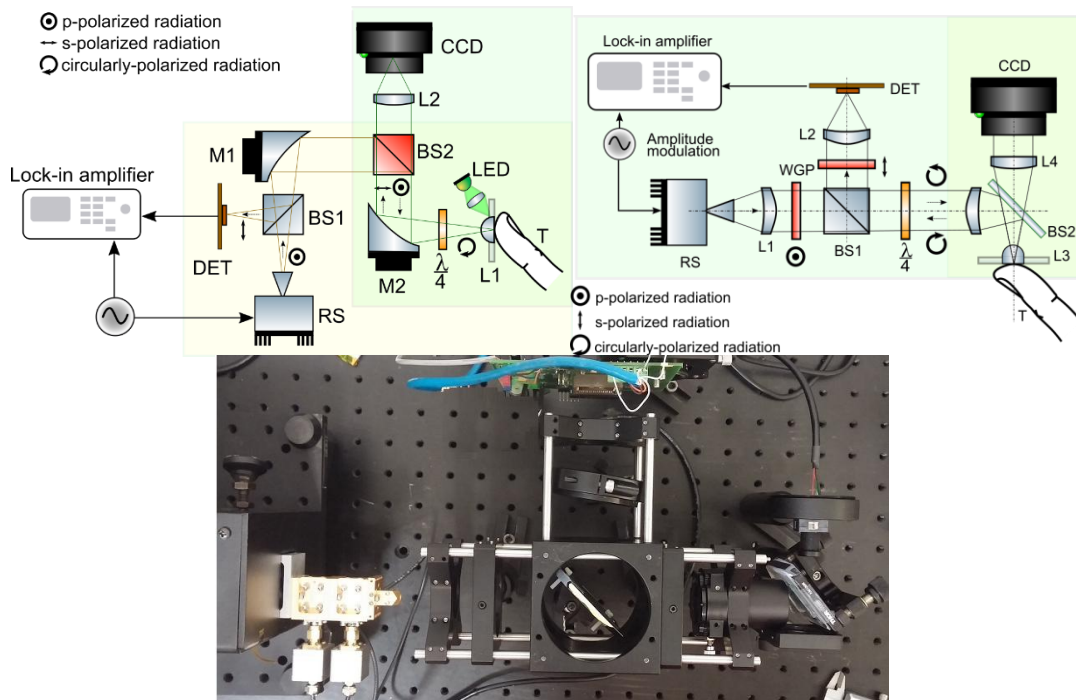
The microscope has been constructed in various forms: multimodal optical and sub-THz imaging at the same time. In order to reach sub-wavelength resolution, we applied solid immersive silicon and sapphire lens, apart from other reflective elements, and glycine to fill up the skin wells. The reached $1-e^2$ resolution is below $\lambda/2$ with numerical aperture 1.3-1.4, which surpasses the optical counterparts.



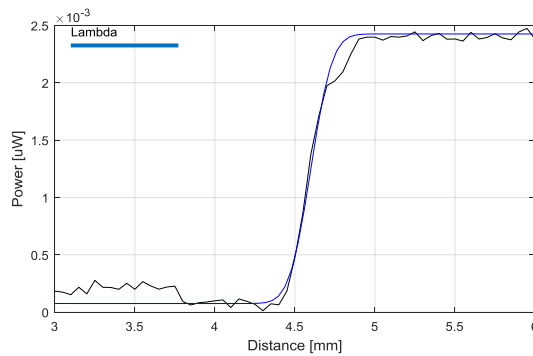
(left) The OCT scan of the skin structure, (middle) ray tracing simulation of the solid state lens structure, (right) EM simulation result including solid state lens and human skin model.

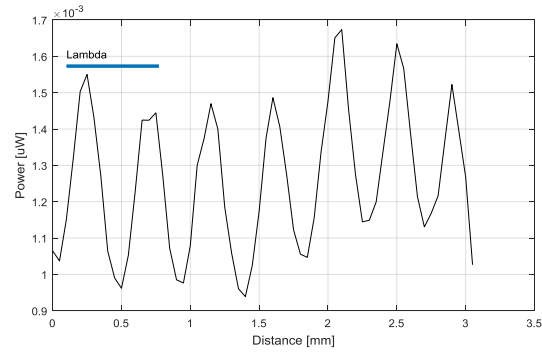
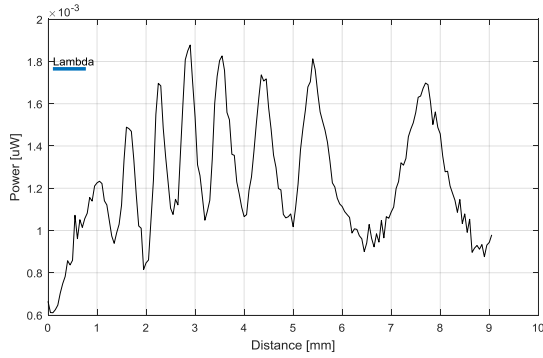
The next figures show the microscope architecture. In the image the RS radiation source provides linearly polarized from 200-520 GHz. The p-polarized radiation goes through the BS1 high resistivity silicon beam splitter and collimated by the M1 off-axis parabolic mirror. The BS2 dichroic beam splitter reflects the radiation towards M2 off-axis parabolic mirror, than focused to the L1 hyperspherical sapphire lens

(the dichronic beam splitter is a boron glass covered by 5 μm indium tin oxide layer). The linear polarization is converted to circular polarization by the quartz quarter-wave plate. The reflected radiation from the target again passes the quarter-wave plate and becomes linearly polarized. Its polarization vector is perpendicular to the source polarization vector. The BS1 beam splitter reflects the majority of the s-polarized reflected radiation and directs the focused beam to the DET detector. In order to avoid low-frequency electrical noise of the detector the radiation is electronically chopped (at 2 kHz) and demodulated after data acquisition. The target area is illuminated by green LED sources and a collimating lens through the acrylic glass diffuser plate. The plate is illuminated by the collimated LED light at two opposite sides to provide even lighting. The visible image is focused by an aspheric lens and captured by a CCD camera. The quarter-wave plate is mounted on a rotating stage to create left- and right-handed circular polarization during measurements.

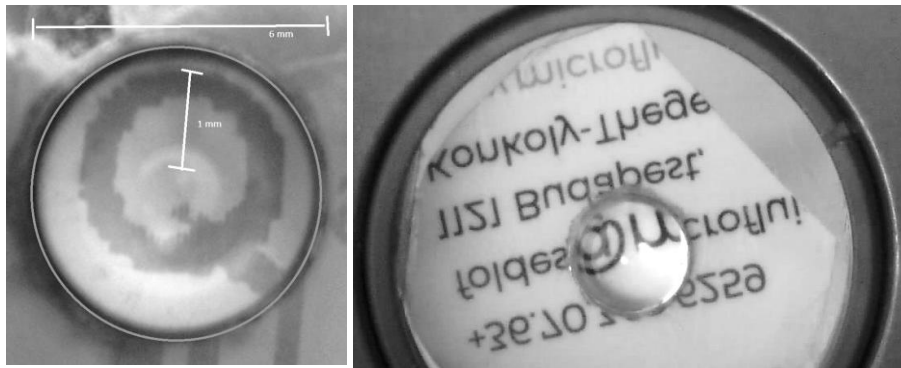


Different arrangements and photo of the multimodal solid state immersion microscope.





Resolution test (top) at $670 \mu\text{m}$ wavelength (460 GHz). The $1 - e^{-2}$ patch size is $250 \mu\text{m}$, that corresponds to about $NA \sim 1.4$ numerical aperture. (lower row) two linear scans of fingers can be seen recorded at 460 GHz.



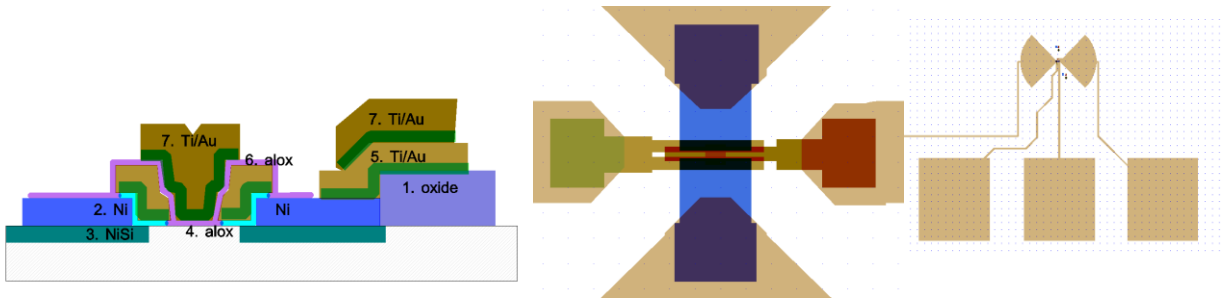
Visible output of the microscope.

Unfortunately, we could not distinguish the sought source, the individual sweat ducts absorption from the average skin absorption. This negative result is more circumstantial to prove and publish, so we continue to work out the identification of the reason for it by e.g. creating skin phantoms.

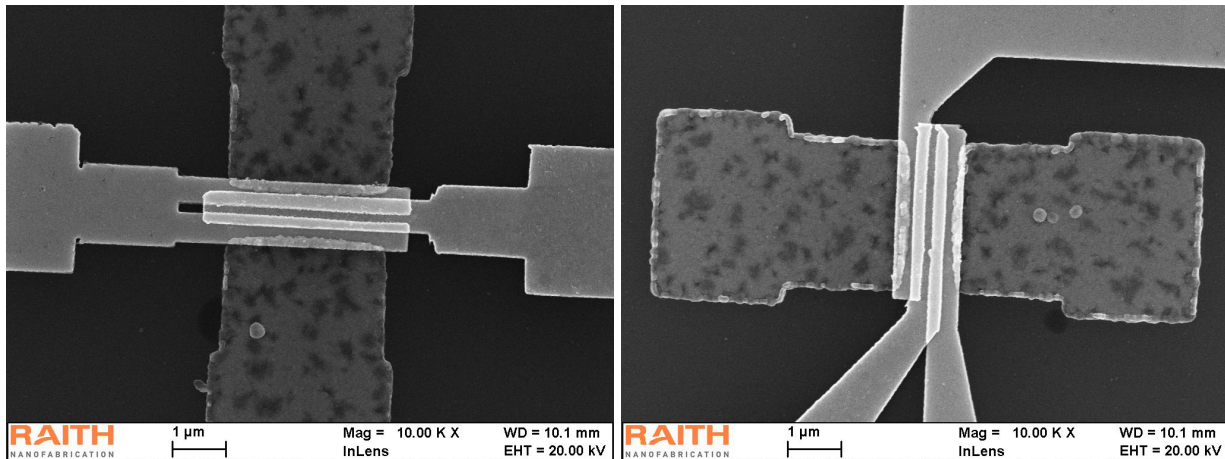
Active metamaterials and detectors

Besides the material based active switching and sensing we have investigated an active device based concept too. From the theoretical work of plasma wave field effect transistor (FET) detection, I have showed that the responsivity can be described by the g_m/I_D (transconductance over drain current) ratio. In order to increase this ratio above the available standard and commercial FETs (limited in silicon to about $30\text{-}40 \text{ V}^{-1}$) we work on low temperature created ultra-steep subthreshold slope FETs and finFETs. Especially on Dual-independent-gate (DIG) silicon FinFETs. This structure were recently shown capable of operating with ultra-steep subthreshold slope of 3.4 mV/dec at room-temperature due to a weak impact ionization induced positive feedback [Zhang, J. et al “A Schottky-Barrier Silicon FinFET with 6.0mV/dec Subthreshold Slope over 5 Decades of Current”, IEDM Tech. Dig., pp. 339-342, 2014.]. Application of a positive voltage on the gate over the source/drain region creates a potential well under the terminal. As voltage is applied on central gate, at the onset of conduction, conducting electrons can acquire enough energy so that electron-hole pairs are generated by impact ionization resulting in a high slope response at the edge of subthreshold region.

Reaching high subthreshold slope rises significantly the g_m/I_D ratio as well with more than an order of magnitude. Thus, our aim is to reproduce dual gate FinFETs in a sensor and possible switching setups. In order to make the structure unique, we have developed a low temperature process flow. The so far reported FETs based on silicon gates and SiO₂ dielectric, which process uses 950-1100 C° degree thermal annealing. On the other hand, our solution uses e-beam defined Ti/Au lift-off gates, Al₂O₃ and HfO₂ dielectric, and contains a single 350 C° degree step to form nickel silicide. All other steps are room temperature processes. Even more to reduce the temperature requirements as an enabling technology, we investigate also the metal-nm range insulator-metal (MIM) ohmic contacting using rare earth element as metal (Erbium) and Al₂O₃ insulator. The solution is not only planned as a THz detector and switching device, but as a sensor for microfluidic environment and biological markers (it is straightforward to make the gold electrodes sensitive and the high subthreshold slope results in high sensitivity). The devices are under THz and electrical measurement at the time of the report.



Cross section and drawn close-up and antenna layout of the dual independent FET defined by Ti/Au lift-off process.



SEM images of the developed dual independent FET. The device consists of a silicon channel, gold source and drain contacts, and two independent gold gate electrodes.

We have prepared two journal papers, which will be submitted as the characterization finished.

The related publication in the period

Földesy Péter, "Integrált érzékelés és jelfeldolgozás a fókusz síkban", MTA Doktora cím eléréséhez benyújtott doktori disszertáció (DSc dissertation). 2017.

Földesy Péter, Z. Fekete, "Multimodal sub-THz circularly polarized scanning microscopy of the human skin duct absorption under physiological conditions", IEEE SENSORS JOURNAL, to be submitted.

Lukács István Endre, Zoltán Fekete, Földesy Péter, "Low temperature process for lift-off defined deep subthreshold slope dual gate FET for sensing applications", IEEE SENSORS JOURNAL, to be submitted.

Gergelyi D, Földesy P, Zarándy Á, „Scalable, Low-Noise Architecture for Integrated Terahertz Imagers”, JOURNAL OF INFRARED MILLIMETER AND TERAHERTZ WAVES 36:(6) pp. 520-536. (2015)

IF: 1.851

Földesy Péter, „Multi-wavelength sub-THz sensor array with integrated lock-in amplifier and signal processing in 90nm CMOS technology”, In: Jung Han Choi, Krzysztof Iniewski (szerk.), High-Speed Devices and Circuits with THz Applications. Boca Raton; Cambridge: CRC Press, 2014. pp. 93-124.

Book chapter

Károlyi G, Gergelyi D, Földesy P, „Sub-Thz Sensor Array with Embedded Signal Processing in 90nm CMOS Technology”, IEEE SENSORS JOURNAL 14:(8) pp. 2432-2441. (2014)

IF: 1.762

Földesy P., „Current steering detection scheme of three terminal antenna-coupled terahertz field effect transistor detectors”, OPTICS LETTERS 38:(15) pp. 2804-2806. (2013)

IF: 3.179

Földesy Péter, „Terahertz responsivity of field-effect transistors under arbitrary biasing conditions”, JOURNAL OF APPLIED PHYSICS 114:(11) Paper 114501. (2013)

IF: 2.185

Földesy P., „Quadrature phase shifted interferometry in the THz spectrum”, 2013 38th International Conference on Infrared, Millimeter, and Terahertz Waves, IRMMW-THz. Konferencia helye, ideje: Mainz, Németország, 2013.09.14-2013.09.19. Piscataway: IEEE, 2013. Paper 6665832. 1 p.

-

Földesy Péter, Gergelyi Domonkos, Kárász Z, Füzy C, „Serially connected MOS terahertz sensor array”, 2013 38th International Conference on Infrared, Millimeter, and Terahertz Waves, IRMMW-THz. Konferencia helye, ideje: Mainz, Németország, 2013.09.14-2013.09.19. IEEE, 2013. Paper 6665576. 2 p.

-

Total impact factor: 8,977

